Published in final edited form as:
J Clin Neurophysiol. 2008 December ; 25(6): 321–330. doi:10.1097/WNP.0b013e31818e8010.

Microphysiology of Epileptiform Activity in Human Neocortex

Catherine A. Schevon[*], **Sau K. Ng**[*], **Joshua Cappell**[†], **Robert R. Goodman**[‡], **Guy McKhann Jr.**[‡], **Allen Waziri**[‡], **Almut Branner**[§], **Alexandre Sosunov**[‡], **Charles E. Schroeder**[‖], and **Ronald G. Emerson**[*,†]

[*]Department of Neurology, Columbia University, New York, New York

[†]Department of Pediatrics, Columbia University, New York, New York

[‡]Department of Neurological Surgery, Columbia University, New York, New York

[§]Cyberkinetics Neurotechnology Systems, Foxboro, Massachusetts

[‖]Department of Psychiatry, Columbia University, New York, New York, U.S.A.

Summary

The authors report the use of dense two-dimensional microelectrode array recordings to characterize fine resolution electrocortical activity ("μEEG") in epileptogenic human cortex. A 16-mm^2 96 microelectrode array with 400-μm interelectrode spacing was implanted in five patients undergoing invasive EEG monitoring for medically refractory epilepsy. High spatial resolution data from the array were analyzed in conjunction with simultaneously acquired data from standard intracranial electrode grids and strips. μEEG recorded from within the epileptogenic zone demonstrates discharges resembling both interictal epileptiform activity ("microdischarges") and electrographic seizures ("microseizures") but confined to cortical regions as small as 200 μm^2. In two patients, this activity appeared to be involved in the initiation or propagation of electrographic seizures. The authors hypothesize that microdischarges and microseizures are generated by small cortical domains that form the substrate of epileptogenic cortex and play important roles in seizure initiation and propagation.

Keywords

Multichannel extracellular recording; Epilepsy; Intracranial EEG; Epileptiform EEG discharges

Recent findings of small (<1 mm^2) foci of high frequency oscillations in both human epilepsy (Bragin et al., 1999,2002) and animal models of epilepsy (Bragin et al., 2000,2002,2003, 2005) suggest that seizures may be initiated in regions comparable in size with basic cortical functional units. It is not known whether epileptiform activity under 40 Hz (i.e., in the frequency range of standard clinical EEG) exhibits similar focality. Although intracranial EEG (iEEG) recordings in patients with intractable epilepsy (Engel et al., 1990;Tonini et al., 2004) afford higher spatial resolution than scalp EEG (Pacia and Ebersole, 1997;Tao et al., 2005), the electrodes used, typically 3 to 5 mm in diameter, effectively sum the electrical potentials generated in large regions of underlying cortex and so cannot register spatial signal patterns at a submillimeter scale. High resolution (~100 μm) recordings spanning cortical layers have been obtained in epilepsy patients using linear array multielectrodes (Ulbert et al., 2004a,

Address correspondence and reprint requests to Catherine A. Schevon, M.D., Ph.D., 710 West 168th Street, New York, NY 10032, U.S.A.; e-mail: cas2044@columbia.edu. .

2004b); this type of electrode can resolve the activity within cortical macro-columns (Schroeder and Seto, 1995) or even microcolumns (Lakatos et al., 2007) but only from one site at a time. High spatiotemporal resolution data from epilepsy patients have also been obtained using bundles of flexible microwires incorporated in a clinical depth electrode with a 1.5-mm tip-to-tip span (Bragin et al., 1999,2002,2003;Worrell et al., 2008), but recording sites are not precisely constrained and spatial resolution is limited. We report results from a two-dimensional, 96-microelectrode array (MEA) in epileptic patients to record neuroelectric signals at high spatial resolution. Our findings demonstrate epileptic abnormalities at a submillimeter scale, including highly focal ictal-appearing events, and provide new insights into the nature of electrophysiological disturbances in human epileptogenic neocortex.

SUBJECTS AND METHODS

Subjects were recruited from patients with medically intractable focal epilepsy undergoing iEEG recording at the Columbia University Medical Center/New York-Presbyterian Hospital to help identify the epileptogenic zone, the tissue that must be removed to obtain seizure control (Rosenow and Luders, 2001). Subjects were limited to patients for whom the presurgical evaluation indicated clear seizure localization to a restricted region and in whom invasive recording was being used to refine the resection boundaries. The study was approved by the Institutional Review Board of the Columbia University Medical Center and informed consent was obtained from each patient.

Microelectrode Array Implantation

The MEA measured 4 mm × 4 mm, and contained 96 microelectrodes (Neuroport neural monitoring system, Cyberkinetics Neurotechnology Systems, Foxboro, MA) arranged in a regular 10 × 10 square with no electrodes at the corner positions. The individual microelectrodes were platinum-coated silicon, protruding 1 mm from the array base and electrically insulated except for the terminal 70 μm. They tapered from 35 to 75 μm in diameter at the base to 3 to 5 μm at their recording tips. Electrode impedance at manufacture was 322 ± 138 kOhm. The MEA was implanted into exposed neocortex through the pia mater using a pneumatic insertion technique (Hochberg et al., 2006; Suner et al., 2005). The implant site was selected based on our estimate of the epileptogenic region from presurgical studies as well as intraoperative corticography, a standard procedure during subdural electrode implantation at our institution. Only flat surfaces of exposed gyri expected to be included in the resection were considered candidate sites for MEA placement; potentially eloquent sites such as Broca's area or primary motor cortex were avoided. After implantation, standard clinical macroelectrode arrays were placed, and contacts nearest the MEA (within 1 cm or partially overlying) were identified. The MEA assembly includes two reference wires; one was placed subdurally near the MEA and the other was placed epidurally. After monitoring, the MEA was explanted along with the standard electrodes.

The epileptogenic zone was defined by the consensus of least two epileptologists at the Columbia Comprehensive Epilepsy Center, based on interictal and ictal intracranial and scalp video-EEG, neuroimaging studies and the results of functional evaluation. The location of the MEA relative to both the cortical surface and the subdural macroelectrodes was identified by intraoperative photographs and frameless stereotactic localization (Brainlab, Westchester, IL), combined with postoperative imaging studies.

Dual Modality Recording

MEA recordings were obtained continuously during video/EEG monitoring, which was performed from 2 days to 2 weeks. We anticipated, based on published prior use of the device for periods as long as 1 year in humans (Hochberg et al., 2006) and nonhuman primates (Suner

et al., 2005) that recording quality would be maintained throughout. Micro-electrode array signals were sampled at 30 kHz/channel (0.3–7.5 kHz bandpass filtering) with 16-bit precision and a range of ±8 mV. The reference signal was selected to optimize recording quality; in each case, it was found that the best results were obtained with the epidural reference. To monitor recording integrity, electrode impedance testing and visual inspection of sample data were performed after the initial hookup and daily thereafter. In addition, the Neuroport system performs online action potential detection (Hochberg et al., 2006); a display of unit activity for each channel, located in the patient's room and remotely accessible by the investigators, served as a real-time monitor of data integrity, allowing recording problems to be remedied quickly.

Intracranial EEG was recorded from standard clinical electrodes (Ad-tech Medical Instrument Corp., Racine, WI or PMT Corp., Chanhassen, MN), 4.0- or 4.5-mm diameter platinum disks spaced 1 cm center to center and arranged in grid or strip arrays. Data were acquired at 500 Hz/channel with 24-bit precision (0.5–125 Hz bandpass filtering) using a standard clinical video-EEG system (XLTek Inc., Oakville, Ontario, Canada). Two contacts of an electrode strip, placed epidurally with electrodes facing away from the dura, served as the reference. Coded sequences of TTL pulses delivered simultaneously to digital inputs of each acquisition system were used to synchronize iEEG and MEA recordings.

Data Processing

Microelectrode array recorded data were downsampled to 500 Hz/channel after antialias filtering at 125 Hz (fourth order Butterworth) to yield high spatial resolution local field potential signals in the frequency range of standard EEG ("μEEG"). Synchronized μEEG and iEEG data were then converted into identical digital formats, merged into combined files, and viewed in spatially organized referential montages using a commercial EEG viewing program (Insight, Persyst Development Corp., Prescott, AZ). Full bandwidth MEA data were retained and the relationship of high frequency components of these data to the μEEG will be reported separately.

Visual Review

The complete combined iEEG/μEEG recording for each patient was reviewed visually. μEEG features morphologically similar to classic interictal and ictal epileptiform abnormalities in standard resolution electroencephalography (Niedermeyer and Lopes da Silva, 1999) were identified visually; we refer to these as "μEDs." μEDs that correlate to epileptiform discharges in the iEEG, and therefore reflect detection of these relatively large scale events by the MEA, are referred to as macrodischarges; μEDs with no correlate in overlying or adjacent clinical electrodes are called microdischarges. Microdischarges occurring in repetitive, evolving temporal patterns similar to ictal events in clinical EEG recordings are referred to as microseizures. The combined iEEG/μEEG data were reviewed independently by two neurophysiologists (C.S. and R.E.) and μED features present were classified and tabulated (Table 2). In the case of conflicting interpretations, a joint review was conducted and the more conservative interpretation agreed upon.

A representative 5-minute recording from each patient was selected for detailed analysis to quantify the occurrence of interictal μEEG features. These samples were chosen from the first day of recording excluding periods within 2 hours of a seizure, such that no movement or other recording artifact was present. For patient 4, who had seizures every 10 to 40 minutes, a recording sample was selected halfway between two seizures occurring 30 minutes apart. Recordings were reviewed independently by two neurophysiologists (C.S. and R.E.) and in the case of disagreement the most conservative count was accepted. The overall concordance rate was 98%.

Statistical Analysis

In the two patients with interictal microseizures (patients 2 and 4), a line-length metric that has been used in seizure detection algorithms (Duckrow and Tcheng, 2007; Esteller et al., 2001) was used to quantify microseizures over a 2-hour period that included at least one clinical seizure. Line length was computed for selected μEEG channels containing microseizures over nonoverlapping 5-second time windows after bandpass filtering (2–20 Hz) to remove high frequency components and low frequency shifts. For each microseizure type, the channel in which the microseizure activity was highest in voltage was selected for line length analysis. For statistical calculations, the resulting vector of line length values was normalized by a control channel at least two channels (0.8 μm) away from the nearest microdischarge to correct for the contribution of macrodischarges. For patient 2, normalized line length vectors computed from three 15-minute periods (interictal 2 hours before seizure onset, preictal ending at seizure onset, and postictal) were used to determine the significance of differences in the means of the line length for preictal and postictal periods compared with the interictal period using the two-sided Wilcoxon rank sum test. In patient 4, because of the frequency of the seizures, line length was compared for 5-minute pre- and postictal periods. All computations were implemented using MAT-LAB (Mathworks, Natick, MA).

RESULTS

MEA recordings were obtained from five patients, two men and three women, between July of 2006 and January of 2007. Their ages ranged from 25 to 41 years (mean 33 years, Table 1). Patient 1 had no seizures in the 2 weeks of monitoring; determination of the epileptogenic zone was based on interictal findings and other clinical data. The MEA implant site was located within the epileptogenic zone in all but patient 1. In patient 1, and also in patient 5, where intracranial recording was performed to tailor temporal lobectomy, the MEA implantation sites were selected such that they would be included in the most conservative resection choices. Complete resection of the epileptogenic zone was accomplished in four of the five patients (Table 1). In patient 3, it was elected to treat the epileptogenic zone with multiple subpial transections, in part, because of the discovery of additional epileptogenic regions in temporal and parietal lobes. Accordingly, in all subjects, the MEA implant site was either resected or treated with multiple subpial transections.

Intracranial EEG recording began on the day of implantation and μEEG recording commenced on postoperative day 1. Recordings continued to the day of explantation. Except for brief (<2 hour) interruptions due to dressing changes, bathroom use, etc., recording quality was excellent throughout. The MEA remained in place in each case, as indicated by the consistent μEEG appearance and real-time unit detections, and confirmed by inspection of the implant site and array at explantation. The number of MEA channels containing excessive artifact, determined by a combination of impedance testing and visual review, was at most 17 (for patient 3), with an average of 8.2 channels per patient. In each case, these channels were apparent when the recording began and no additional artifact channels appeared subsequently.

Interictal Epileptiform Activity

Microdischarges were recorded in four of five patients (Table 2 and Figs. 1-3). These discharges were notable for their limited spatial extents of from 1 to 18 contiguous electrode sites, encompassing a cortical surface area of 0.2 to 4 mm^2, based on visual identification in the μEEG at a display gain corresponding to 150 μV/mm. We found no examples of μEDs that covered an area larger than 4 mm^2 but smaller than the entire MEA. Although μEDs, occupying an area of 4 mm^2 or less, were never detected in iEEG even at electrode sites immediately adjacent to or overlying the MEA, when μEDs were seen in the entire MEA they correlated with iEEG discharges 97% (482/497) of the time.

Microseizures

In three patients, the μEEG contained patterns not reflected in the iEEG that resembled electrographic seizures (Table 2). These consisted of runs of repetitive sharp waveforms or continuous rhythmic activity, at times evolving in frequency, amplitude, and morphology, i.e., properties that characterize electrographic seizures in conventional EEG recordings (Niedermeyer and Lopes da Silva, 1999) (Fig. 1). We refer to these discharge patterns as "microseizures" to distinguish them from electrographic seizures commonly recognized in standard clinical intracranial recordings.

In patient 2, microseizures were present in four distinct regions within the MEA (Table 2; Fig. 1). They developed after the first 24 hours of recording and were observed over the subsequent 36 hours. During this period, microseizures appeared to wax and wane and were not associated with behavioral changes. These microseizures remained confined to specific microelectrodes in the MEA and did not spread to other microelectrodes. Although microseizures were not observed to lead directly to an electrographic seizure in the iEEG, microseizure activity, as estimated by normalized line length as described in Methods section, increased significantly preictally and fell significantly following a clinical seizure in three of the four sites tested (two-sided Wilcoxon rank sum test, $P < 0.01$) (Fig. 4). Although microseizures were observed only during the initial 60 hours of recording, microdischarges were present in these same regions throughout the entire 5 days of monitoring.

Microseizures were prominent in the μEEG of patient 4, who had recurrent partial seizures every 10 to 40 minutes. Beginning immediately following the termination of each clinical seizure, periodic microdischarges increased steadily in amplitude, frequency, and distribution, developing into a microseizure. This buildup was gradual and was independent of frequent, irregularly occurring, epileptiform discharges in the iEEG. It preceded apparent "seizure onset" in the iEEG, which occurred at either of two distinct seizure onset sites, each ~4 cm from the MEA. Just before seizure offset, electrographic seizure discharges in iEEG and microseizure discharges in the MEA became synchronized (Fig. 2D).

In patient 5, with clinical and electrographic findings consistent with mesial temporal lobe epilepsy, microseizures were seen only during recruitment of the MEA implantation site in lateral temporal cortex into an ongoing seizure (Fig. 3). Ictal onset appeared in the iEEG as a burst of high frequency activity in the subtemporal strips. It was followed within 1 second by periodic, ~2 Hz, simply configured discharges in both subtemporal and lateral temporal cortex, and by approximately synchronous macrodischarges in the MEA (Fig. 3B). Approximately 7 seconds after ictal onset, an independent microseizure characterized by focal, semirhythmic beta range activity appeared abruptly and simultaneously in two separate regions of the array. This activity was confined initially to five microelectrodes and then spread rapidly to engulf the entire MEA. Interestingly, frequent microdischarges were observed interictally at these same sites (Fig. 3A).

DISCUSSION

Intracortical MEA recordings reveal features of EEG with unprecedented spatial resolution. The regular two dimensional geometry of the MEA permits spatial information to be preserved in a manner not possible with either individual linear array multielectrodes (Ulbert et al., 2004) or with flexible microwire bundles (Bragin et al., 1999). Interelectrode spacing of 400 μm makes it possible to resolve electrophysiological events at the scales of anatomic and physiological microdomains (Bartfeld and Grinvald, 1992; Horton and Hocking, 1996; Mountcastle, 1997). We recorded microdischarges from areas of 0.2 mm^2 (i.e., detected in only single microelectrodes) to up at most 4mm^2. Although comparable in voltage with macrodischarges seen in the MEA, EDs, and iEEG, microdischarges were never detected by

adjacent or partially overlying iEEG electrodes. It is likely that the currents arising from their small generators are insufficient to observably influence voltages detected by standard iEEG electrodes, which sample from cortical areas of about 12 mm^2. Moreover, the MEA appears capable of resolving a rich complexity of spatially restricted asynchronous signals from neighboring microdomains; in the iEEG these signals would simply summate or cancel.

Key Findings and Emergent Questions

Observations made possible by the spatial resolution provided by the MEA will likely add to our understanding of the pathophysiology of epilepsy. Of particular interest are the microseizures present interictally in two patients and during seizure propagation in a third. Their waveform morphology and periodicity, and in some cases evolution in frequency and morphology, resembled those of ictal patterns in conventional iEEG recordings. However, microseizures were restricted to one or several disparate foci in the MEA and were never detected by the iEEG.

Do microseizures and microdischarges reflect epileptic abnormalities? It is important to establish whether microdischarges and microseizures are, in fact, abnormal, or whether they are simply previously unrecognized features of normal cortex that are not recordable with standard electrodes. Three lines of evidence support the former view. First, it is unlikely that microdischarges and microseizures are attributable to electrode artifact or reference contamination, as they display consistent voltage fields in sets of adjacent, yet spatially restricted electrodes (e.g., Fig. 1). Second, no microdischarges or microseizures were recorded in the only patient in whom μEEG was sampled from uninvolved, nonepileptogenic cortex. In this case (patient 1), the epileptogenic zone was restricted to mesial temporal structures and the MEA was implanted in the middle temporal gyrus (Table 1). Neither histopathology, presurgical studies, nor clinical electrophysiology implicated the lateral temporal lobe as part of the epileptogenic zone. Microdischarges were recorded from patient 5, who also had mesial temporal epilepsy, but in whom the MEA implantation site was clearly within the epileptogenic zone. This patient demonstrated independent lateral temporal EDs in the contacts adjacent to the MEA implant site. In addition, the MEA was situated within 2 cm of the anterior temporal pole in the inferior temporal gyrus, an area with rich mesial connectivity shown by SPECT (Tae et al., 2005) and diffusion tensor imaging (Thivard et al., 2005). In all patients, in whom the MEA was situated within the epileptogenic zone, both microdischarges and microseizures were recorded. Finally, the limited spatial extent of both microseizures and microdischarges is consistent with the restricted distribution previously demonstrated for high frequency oscillations recorded from human epileptogenic tissue (Bragin et al., 2002) as well as in animal models of epilepsy (Bragin et al., 2003). Any relationship, however, between epileptiform μEEG features and high frequency oscillations remains to be demonstrated. Taken together, the data from this limited case series suggest that microdischarges and microseizures are indeed features of epileptogenic cortex. Data from additional patients recorded both from within and from outside the epileptogenic zone will be required for confirmation.

What is the relationship between microseizures and seizures? The evolution of microseizures, on a millimeter or submillimeter scale, appears to reflect the participation of small regions of cortex in overall seizure evolution. In patient 4, leading up to a clinical seizure, microseizure waveforms increased in amplitude and frequency, spread to involve additional microelectrodes in the MEA and became progressively “sharper” and more complex in morphology. This evolution was independent of the evolving iEEG ictal activity, which appeared to begin at one of two sites, each ~4 cm from the MEA; the iEEG and microseizure finally became entrained just before seizure offset (Fig. 2). In patient 5, the lateral temporal MEA demonstrated two distinct patterns after mesial temporal ictal onset: initially the MEA detected widely distributed

propagated ictal discharges; then, an independent beta frequency microseizure suddenly appeared, likely reflecting secondary involvement of the MEA site in the seizure (Fig. 3).

These observations are consistent with the view, initially proposed by Bragin et al. (2000), that epileptogenic cortex may consist of a network of epileptogenic domains dispersed with fine granularity among a majority of more normally functioning domains. It is attractive to speculate that microdischarges and microseizures, as markers of epileptogenic cortex, represent seed events for the initiation and propagation of interictal discharges and seizures. In this model, epileptogenic domains as small as single cortical columns (Mountcastle, 1997) and surrounded by nonepileptogenic tissue may give rise to these protoepileptic events. Clinical seizures may occur when a microseizure spreads to involve adjacent nonepileptogenic tissue, perhaps involving the activation and synchronization of a functionally connected network of epileptogenic domains. These hypotheses are consistent with previous proposals, based on hippocampal microelectrode recordings in an animal models of epilepsy, that small neuronal aggregates can serve as a substrate for epileptogenesis and seizure initiation (Bikson et al., 2003; Bragin et al., 2000). However, because the MEA records only a small cortical area (16 mm^2), the chance of directly observing this phenomenon is likely to be small and in our patients, this was, in fact, not observed.

Implications for Surgical Management of Focal Epilepsy

Current methods of electrocorticographic identification of epileptogenic tissue have important limitations. Neural conduction contributes to the apparent “fields” of EDs in standard recordings (Emerson et al., 1995); as such, it is possible that the “presence” of epileptiform activity at a given site may not per se be strong evidence that the site is capable of independently generating this activity. Resection of secondarily involved cortical areas may not contribute to post-surgical seizure control and could unnecessarily compromise function. Conversely, primary epileptogenic cortex may not always be apparent in traditional clinical recordings. This was potentially the case in patient 4, where the μEEG pattern suggested early involvement of the MEA site in the process of seizure evolution but was not seen in the iEEG. It is possible that μEEG may supplement information provided by conventional techniques leading to more accurate identification of epileptogenic tissue. If, as we suspect, microseizures are signatures of epileptogenic cortex, methods with the spatial sampling ability of the MEA used here could contribute to effective, yet conservative definition of areas to be resected.

Acknowledgments

The authors acknowledge the epilepsy faculty of Columbia University Department of Neurology who contributed to the clinical evaluation of the patients in this study, including Carl Bazil, Hyunmi Choi, Derek Chong, Frank Gilliam, Lawrence Hirsch, Steven Karceski, Anil Mendiratta and Alison Pack. Funding for this work was provided by the National Institute of Neurologic Disorders and Stroke (K08 NS48871, CAS). Equipment and technical support was provided by Cyberkinetics Neurotechnology Systems, Inc.

REFERENCES

1. Bartfeld E, Grinvald A. Relationships between orientation-preference pin-wheels, cytochrome oxidase blobs and ocular-dominance columns in primate striate cortex. Proc Natl Acad Sci USA 1992;89:11905–11909. [PubMed: 1465416]
2. Bikson M, Fox JE, Jefferys JG. Neuronal aggregate formation underlies spatiotemporal dynamics of nonsynaptic seizure initiation. J Neurophysiol 2003;89:2330–2333. [PubMed: 12686586]
3. Bragin A, Azizyan A, Almajano J, et al. Analysis of chronic seizure onsets after intrahippocampal kainic acid injection in freely moving rats. Epilepsia 2005;46:1592–1598. [PubMed: 16190929]
4. Bragin A, Engel J Jr, Wilson CL, et al. High-frequency oscillations in human brain. Hippocampus 1999;9:137–142. [PubMed: 10226774]

5. Bragin A, Mody I, Wilson CL, et al. Local generation of fast ripples in epileptic brain. J Neurosci 2002;22:2012–2021. [PubMed: 11880532]
6. Bragin A, Wilson CL, Engel J Jr. Chronic epileptogenesis requires development of a network of pathologically interconnected neuron clusters: a hypothesis. Epilepsia 2000;41(suppl 6):S144–S152. [PubMed: 10999536]
7. Bragin A, Wilson CL, Engel J. Spatial stability over time of brain areas generating fast ripples in the epileptic rat. Epilepsia 2003;44:1233–1237. [PubMed: 12919396]
8. Bragin A, Wilson CL, Staba RJ, et al. Interictal high-frequency oscillations (80–500Hz) in the human epileptic brain: entorhinal cortex. Ann Neurol 2002;52:407–415. [PubMed: 12325068]
9. Duckrow RB, Tcheng TK. Daily variation in an intracranial EEG feature in humans detected by a responsive neurostimulator system. Epilepsia 2007;48:1614–1620. [PubMed: 17442001]
10. Emerson RG, Turner CA, Pedley TA, et al. Propagation patterns of temporal spikes. Electroencephalogr Clin Neurophysiol 1995;94:338–348. [PubMed: 7774520]
11. Engel J, Henry TR, Risinger MW, et al. Presurgical evaluation for partial epilepsy: relative contributions of chronic depth-electrode recordings versus FDG-PET and scalp-sphenoidal ictal EEG. Neurology 1990;40:1670–1677. [PubMed: 2122275]
12. Esteller, R.; Echauz, J.; Tcheng, T., et al. Line length: an efficient feature for seizure onset detection. Proceedings of the 23rd Annual International Conference of the IEEE Engineering in Medicine and Biology Society; Istanbul, Turkey. 2001. p. 1707-1710.
13. Hochberg LR, Serruya MD, Friehs GM, et al. Neuronal ensemble control of prosthetic devices by a human with tetraplegia. Nature 2006;442:164–171. [PubMed: 16838014]
14. Horton JC, Hocking DR. Intrinsic variability of ocular dominance column periodicity in normal macaque monkeys. J Neurosci 1996;16:7228–7239. [PubMed: 8929431]
15. Lakatos P, Chen CM, O'Connell MN, et al. Neuronal oscillations and multisensory interaction in primary auditory cortex. Neuron 2007;53:279–292. [PubMed: 17224408]
16. Mountcastle VB. The columnar organization of the neocortex. Brain 1997;120:701–722. [PubMed: 9153131]
17. Niedermeyer, E.; da Silva, F Lopes. Electroencephalography: Basic Principles, Clinical Applications and Related Fields. Lippin-cott Williams & Wilkins; Baltimore, MD: 1999.
18. Pacia SV, Ebersole JS. Intracranial EEG substrates of scalp ictal patterns from temporal lobe foci. Epilepsia 1997;38:642–654. [PubMed: 9186246]
19. Rosenow F, Luders H. Presurgical evaluation of epilepsy. Brain 2001;124(pt 9):1683–1700. [PubMed: 11522572]
20. Schroeder CE, Seto S. Electrophysiologic evidence for overlapping dominant and latent inputs to somatosensory cortex in squirrel monkeys. J Neurophysiol 1995;74:722–32. [PubMed: 7472377]
21. Suner S, Fellows MR, Vargas-Irwin C, et al. Reliability of signals from a chronically implanted, silicon-based electrode array in non-human primate primary motor cortex. IEEE Trans Neural Syst Rehabil Eng 2005;13:524–541. [PubMed: 16425835]
22. Tae WS, Joo EY, Kim JH, et al. Cerebral perfusion changes in mesial temporal lobe epilepsy: SPM analysis of ictal and interictal SPECT.". Neuroimage 2005;24:101–110. [PubMed: 15588601]
23. Tao JX, Ray A, Hawes-Ebersole S, et al. Intracranial EEG substrates of scalp EEG interictal spikes. Epilepsia 2005;46:699–676.
24. Thivard L, Lehericy S, Krainik A, et al. Diffusion tensor imaging in medial temporal lobe epilepsy with hippocampal sclerosis. Neuroimage 2005;28:682–690. [PubMed: 16084113]
25. Tonini C, Beghi E, Berg AT, et al. Predictors of epilepsy surgery outcome: a meta-analysis. Epilepsy Res 2004;62:75–87. [PubMed: 15519134]
26. Ulbert IG, Heit G, Madsen J, et al. Laminar analysis of human neocortical interictal spike generation and propagation: current source density and multiunit analysis in vivo. Epilepsia 2004a;45(suppl 4): 48–56. [PubMed: 15281959]
27. Ulbert IZ, Magloczky Z, Eross L, et al. In vivo laminar electrophysiology co-registered with histology in the hippocampus of patients with temporal lobe epilepsy. Exp Neurol 2004b;187:310–318. [PubMed: 15144857]

28. Worrell GA, Gardner AB, Stead SM, et al. High-frequency oscillations in human temporal lobe: simultaneous microwire and clinical macroelectrode recordings. Brain 2008;131:928–937. [PubMed: 18263625]

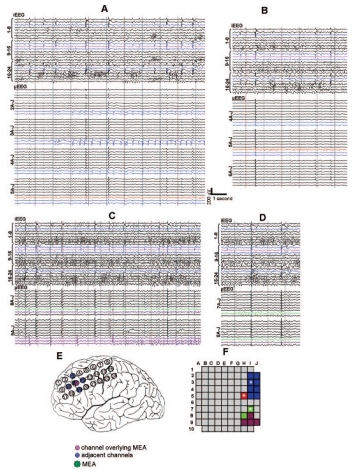

FIGURE 1.

Examples of interictal microseizure activity. μEEG is shown illustrating four morphologically and topographically distinct microseizures (panels **A**—**D**) recorded from patient 2, shown along with synchronized iEEG. Intracranial EEG electrode locations are illustrated on the implant schematic (panel **E**). In panels **A**—**E**, iEEG electrode 11, partially overlying the MEA, is shown in pink; the surrounding iEEG electrodes are highlighted in blue. μEEG channels are organized by rows and columns as shown in the MEA schematic (panel **F**). μEEG channels containing microseizures are color-coded blue, red, green and purple corresponding to distinct regions of the MEA (panel **F**). Microelectrode locations marked by asterisks in panel **F** designate channels studied in the line length calculations of Figure 4. Note that each microseizure is localized to a distinct domain and none has an iEEG correlate. Conversely, iEEG discharges seen in the lateral frontal grid appear throughout the MEA as high amplitude, widely distributed μEEG discharges with a consistent morphology.

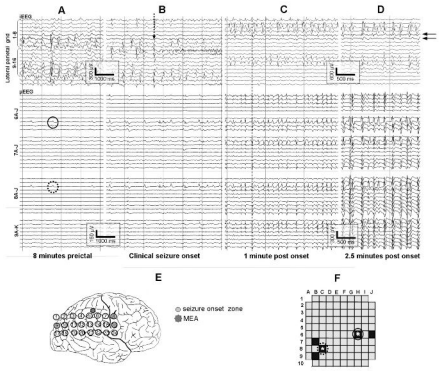

FIGURE 2.

Microseizure development correlating with a clinical seizure. Four segments of synchronized iEEG/μEEG recordings from patient 4, showing progressive buildup of a microseizure in the MEA, which merges with a seizure in adjacent iEEG electrodes (panels **A**—**D**). Intracranial EEG is shown from three rows of the lateral parietal grid, placed as shown in the implant schematic (panel **E**). The location of the channels closest to the MEA is indicated by arrows on the right edge of panel **D**. Immediately after the previous seizure (and 8 minutes before the onset of the illustrated seizure), the microdischarges first appear as sharp waves and brief bursts of low amplitude beta activity seen predominantly in five electrodes located <1 mm from one another (panel **F**, darkened microelectrode sites), recurring at about 0.3 to 1 Hz (panel **A**, circles). These microdischarges increase in voltage and frequency, recurring at up 2 Hz (panel **B**) and subsequently spread to involve other, at times noncontiguous, MEA electrode locations (panel **C**). Seizure onset in the iEEG appears to begin 4 cm from the MEA in channel 9 (panel **B**, dashed arrow); this was typical of 2/3 (27 of 45) of the recorded seizures, whereas the rest appeared to begin in channel 8 and 16, a similar distance away. μEDs continue to increase in frequency, but remain asynchronous with iEEG ictal discharges 60 seconds after iEEG seizure onset (panel **C**, vertical dashed line). The microseizure finally becomes synchronized with iEEG ictal activity just before ictal offset, 150 seconds after seizure onset (panel **D**).

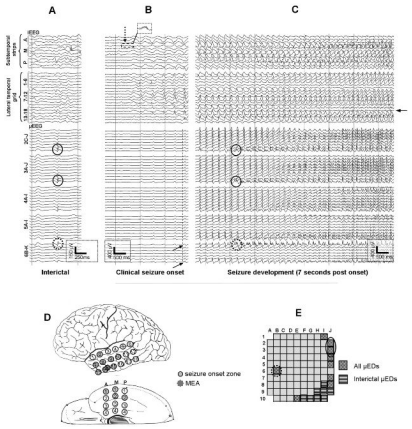

FIGURE 3.

Seizure propagation initiating a microseizure. Selected channels of synchronized iEEG/μEEG recordings from patient 5 are illustrated, showing ictal onset in subtemporal electrodes, and subsequent recruitment of a lateral temporal region recorded by the MEA with a microseizure. The microseizure starts in a subset of channels that were most active interictally. Intracranial EEG channel 14 partially overlies the MEA (panel **D**; arrow to the right of panel **C**). Intracranial EEG channels from the lateral temporal grid and subtemporal strips are shown in the implant schematic (panel **D**); inferior temporal channels are grouped as shown in panel **D**, each group ordered top down, starting from electrode 1. Panel **A** shows a microdischarge with no accompaniment in the iEEG. The complex architecture of the microdischarge is evident, with highly restricted topography and supimposed beta frequency activity (black circles). In panel **B**, ictal onset (vertical dashed arrow) is seen in the subtemporal strips as high frequency activity (shown in the enlarged view), and is followed by 2 to 2.5 Hz discharges in mesial and lateral temporal iEEG electrodes. These are registered by the MEA as well. Close examination of the μEDs comprising the seizure discharges reveals highly focal variations in waveshape (solid black arrows) and timing (dashed vertical line); this excludes a significant contribution by volume conduction and instead is consistent with neural conduction of ictal discharges to the array. Seven seconds after seizure onset (circles, panel **C**), a microseizure emerges, appearing as semirhythmic beta range activity in the channels that previously demonstrated interictal microdischarges (panel **A**), and then continues to spread throughout the MEA.

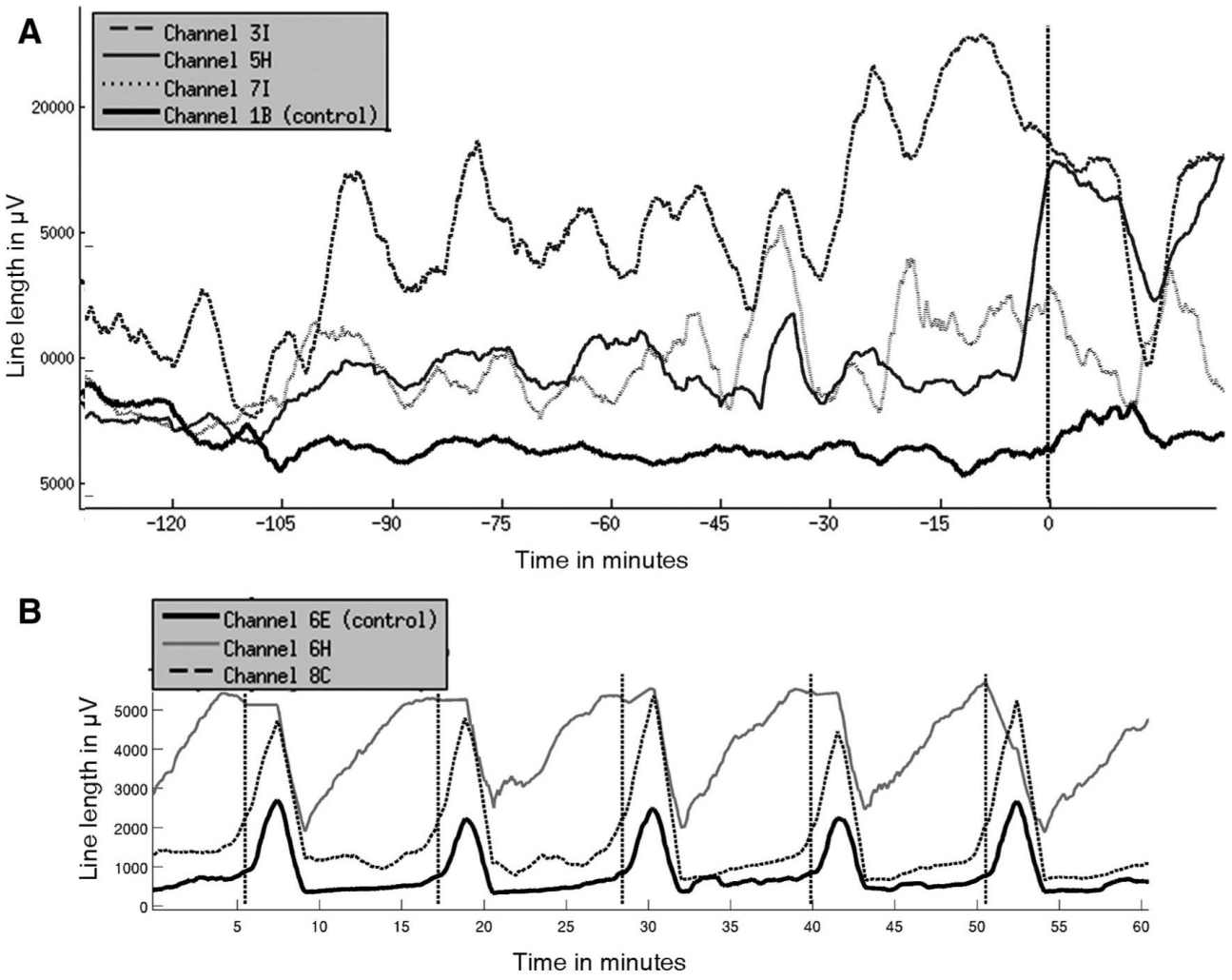

FIGURE 4.

Line length measure of microseizures. **A**. Interictal microseizure activity, measured by line length, in patient 2 over a 2-hour period leading up to a seizure is illustrated for microelectrode channels in three different microseizure domains within the MEA (dashed gray line, channel 3I in the blue region; solid gray line, channel 5H in the red region, and dotted line, channel 7I in the green region; see Fig. 1, panel **F**). Line length calculated from a control microelectrode 1B, exhibiting no microseizures, serves as a control (heavy black line). In comparison with the control channel, microseizure activity begins to increase beginning about 100 minutes before the clinical seizure (vertical dashed line) compared with the initial recording segment, and decreases postictally. The preictal line length values were significantly different from those in the first 15 minutes of this recording segment, as were the postictal line length values when compared with preictal for the three channels shown (two-sided Wilcoxon rank sum test, $P < 0.05$). **B**, Microseizure activity over a 1 hour period in patient 4 that included five distinct clinical seizures. Channels recorded from within MEA regions with microseizures (asterisks in Fig. 2**F**) behave differently than the control channel; the effect is most prominent in channel 6H (solid gray line). In both cases, there is a steady increase in line length that begins almost immediately after the previous seizure and shows a consistent relationship with seizure onset times (vertical dashed lines).

TABLE 1

Clinical Summary

Patient	Implant Location	MEA Location	Epileptogenic Zone	No. Days	No. Seizures	Pathology	Outcome (Follow-up Time)
1 (41 F)	Right lateral and subtemporal	Right middle temporal gyrus 4 cm from anterior temporal tip	Right mesial temporal (based on interictal data)	13	0	Focal reactive leptomeningitis under MEA; no MTS; no dysplasia	Engel Ia (1 yr)
2 (39 M)	Left lateral and mesial frontal	Left lateral frontal, minimum distance 1.5 cm superior to Broca's area and on different gyrus	Left frontal operculum (3 × 3 cm cortical area)	4	7	Chaslin's subpial gliosis; electrode tips in layer IV	Engel 1a (6 mo)
3 (30 M)	Left lateral frontal, mesial frontal, temporal	Left lateral frontal, minimum distance 2 cm superior to Broca's area and on different gyrus	Boundaries not defined but maximal area identified in left lateral frontal lobe	4	~50	N/A (MST only)	Engel III (10 mo)
4 (30 F)	Right parietal including central sulcus, extending back to occipital lobe and inferiorly to posterior temporal region	Superior right parietal, 4 cm posterior to central sulcus	Right parietal (8 × 2 cm cortical area)	2	~80	Chaslin's subpial gliosis	Engel Ib (11 mo)
5 (25 F)	Left lateral and subtemporal	Left inferior temporal gyrus 2.5 cm from anterior temporal tip	Left mesial and anterolateral temporal	5	3	Mild CA1 neuronal loss, Chaslin's subpial gliosis in anterior temporal lobe, electrode tips in layers IV–V	Engel 1a (6 mo)

Summary of clinical data for the five patients chronically implanted with the Neuroport MEA, including the locations of the clinical and MEA implants, the number of days of chronic recording from the MEA, and the location of the epileptogenic zone determined after intracranial monitoring. Patient 4 had partial seizures lasting 1–3 min and occurring every 10–40 min in a cyclic pattern throughout the 40-h monitoring period. Patient 3 also had a large number of recorded seizures. These were brief tonic seizures that occurred in nine distinct clusters with up to 15 seizures each. The epileptogenic zone in patient 3 included large areas of the frontal and temporal lobes. Multiple subpial transections (MSTs) were carried out in an area of the lateral frontal cortex that included the MEA implant location. Outcome following resection is included for all five patients; follow-up times range from 6 mo to 1 yr. Pathology results from examination of the resected tissue are described where applicable.

MEA, microelectrode array.

TABLE 2

Summary of Interictal μEEG and iEEG Patterns

Patient	Principal EEG Patterns Present, as Recorded Simultaneously in:				Five-Minute Interictal Pattern Count		
	μEEG						
		Maximum No. Electrodes	No. Patterns	iEEG	Both	iEEG Only	μEEG Only
1	No correlate	—	—	Mesial temporal EDs	—	26	—
2	Macrodischarges	—	—	Parietal EDs	147	306	0
	Microdischarges	4	1	No correlate	—	—	121
	Microseizures	—	1	No correlate	Evolution and spread before each seizure		
3	Macrodischarges	—	—	Lateral frontal EDs <1 cm from MEA	25	—	—
	Macrodischarges	—	—	Lateral frontal EDs >1 cm from MEA	1	4	0
	Microdischarges	18	3	No correlate			22
4	Macrodischarges	—	—	Lateral frontal EDs	264	0	14
	Microdischarges	6	6	No correlate	—	—	>400
	Microseizures	—	4	No correlate	Frequent runs with evolution, 2 s to 2 min		
5	Macrodischarges	—	—	Mesial temporal EDs	39*	20	0
	Macrodischarges	—	—	Lateral temporal EDs	6	0	1
	Microdischarges	16	1	No correlate	—	—	2
	Microseizures	—	1	No correlate	Seen as propagation pattern during clinical seizures		

Interictal epileptiform μEEG and iEEG patterns identified in each of the five patients based on review of the entire record, along with discharge counts in a 5-min recording sample containing all μED types but not microseizures. Each line of the table describes the appearance of the pattern in the μEEG (microdischarge, macrodischarge, or microseizure) and iEEG, and the number of times the pattern occurred in each modality. For simplicity, distinct microdischarge and microseizure patterns are reported together, with the number of pattern types indicated. For microdischarges and microseizures, the maximum number of electrodes involved for each patient is shown, to indicate the largest area of involvement. “No correlate” indicates that particular pattern was never seen in the modality indicated. Macrodischarges were seen in all patients; microdischarges were seen in patients 2 to 5. The frequency of microdischarges was highly variable; the ratio of the number of microdischarges to macrodischarges varied from 3% (patient 5) to 151% (patient 4). In patient 1, all macrodischarges were distant to the MEA location (in the mesial/subtemporal region), and no microdischarges or macrodischarges were detected in the μEEG.

MEA, microelectrode array; iEEG, intracranial EEG.

*In nine cases, low-voltage EDs were detected in lateral temporal iEEG electrodes as well as the MEA.